Available online at www.sciencedirect.com
SCIENCE DIRECT®
Applied Radiation and Isotopes 62 (2005) 25–32
Applied Radiation and Isotopes
www.elsevier.com/locate/apradiso

Application of deuteron–deuteron (D–D) fusion neutrons to $^{40}Ar/^{39}Ar$ geochronology

Paul R. Renne[a,b,*], Kim B. Knight[b], Sébastien Nomade[a,b], Ka-Ngo Leung[c,d], Tak-Pui Lou[c,d]

[a] *Berkeley Geochronology Center, 2455 Ridge Road, Berkeley, CA 94709, USA*
[b] *Department of Earth and Planetary Science, University of California, Berkeley, CA 94720, USA*
[c] *Division of Accelerator and Fusion Research, Lawrence Berkeley Laboratory, One Cyclotron Road, Berkeley, CA 94720, USA*
[d] *Department of Nuclear Engineering, University of California, Berkeley, CA 94720, USA*

Received 15 March 2004; received in revised form 10 June 2004; accepted 11 June 2004

Abstract

Neutron irradiation of samples for $^{40}Ar/^{39}Ar$ dating in a ^{235}U fission reactor requires error-producing corrections for the argon isotopes created from Ca, K, and, to a lesser extent, Cl. The fission spectrum includes neutrons with energies above 2–3 MeV, which are not optimal for the $^{39}K(n,p)^{39}Ar$ reaction. These higher-energy neutrons are responsible for the largest recoil displacements, which may introduce age artifacts in the case of fine-grained samples. Both interference corrections and recoil displacements would be significantly reduced by irradiation with 2.45 MeV neutrons, which are produced by the deuteron–deuteron (D–D) fusion reaction $^{2}H(d,n)^{3}He$. A new generation of D–D reactors should yield sufficiently high neutron fluxes ($>10^{12}$ n cm^{-2} s^{-1}) to be useful for $^{40}Ar/^{39}Ar$ dating. Modeling indicates that irradiation with D–D neutrons would result in scientific benefits of improved accuracy and broader applicability to fine-grained materials. In addition, radiological safety would be improved, while both maintenance and operational costs would be reduced. Thus, development of high-flux D–D fusion reactors is a worthy goal for $^{40}Ar/^{39}Ar$ geochronology.

Keywords: Deuteron; Fusion; Neutron; Argon; Geochronology

Introduction

The $^{40}Ar/^{39}Ar$ dating method (Merrihue and Turner, 1966) is the most widely applicable geochronometer available for measuring geologic time. It is unique among radioisotopic dating methods in being applicable over time scales ranging from that of the early solar system (4.5 billion years ago) to that of *Homo sapiens*, extending even into the recorded history (Renne et al., 1997). The method is based on the electron-capture decay of ^{40}K to ^{40}Ar. It utilizes neutron activation of ^{39}K to ^{39}Ar via the $^{39}K(n,p)^{39}Ar$ reaction as a proxy for the parent isotope ^{40}K in light of the general invariance of $^{39}K/K$ in nature (Garner et al., 1975; Humayun and Clayton, 1995). This approach makes possible mass-spectrometric measurements of the parent proxy (^{39}Ar) and the daughter (^{40}Ar) from the same sample. The neutron activation is conventionally achieved by irradiating samples in the core of a ^{235}U fission reactor, where they are bombarded by neutrons of a broad spectrum of energies. The $^{39}K(n,p)^{39}Ar$ cross section increases sharply between 1.5 and 3.0 MeV, and, in a typical fission reactor, approximately 50% of the ^{39}Ar nuclides are produced by neutrons with energies greater than 3 MeV (Fig. 1).

The pioneers of $^{40}Ar/^{39}Ar$ dating (e.g., Turner, 1971) recognized that, in geological samples, the fission-spectrum neutrons produce, along with the desired

*Corresponding author. Tel.: +1-510-644-9200; fax: +1-510-644-9201.
E-mail address: prenne@bgc.org (P.R. Renne).

0969-8043/$ - see front matter © 2004 Elsevier Ltd. All rights reserved.
doi:10.1016/j.apradiso.2004.06.004

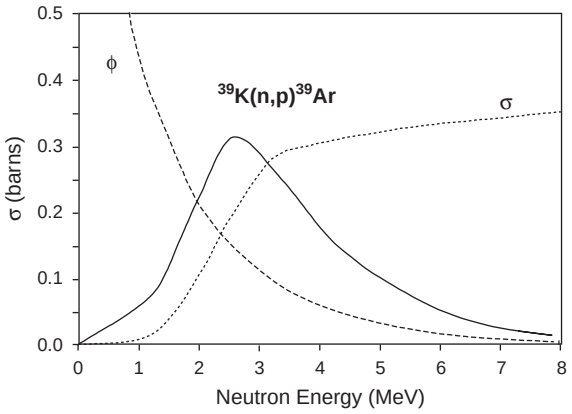

Fig. 1. Cross section of the ^{39}K(n,p) ^{39}Ar reaction as a function of the neutron energy. The figure also shows relative neutron flux (ϕ, arbitrary units) for the CLICIT facility of the TRIGA reactor at OSU. The product of the two functions (solid curve labeled ^{39}K(n,p) ^{39}Ar) gives the relative production of ^{39}Ar as a function of the neutron energy.

reaction ^{39}K(n,p) ^{39}Ar, many unwanted processes. In particular, the argon isotopes produced by the reactions on isotopes of K, Ca, and Cl require corrections, so that the ^{40}Ar/^{39}Ar age equation could be meaningfully applied to argon isotope data. A summary of these interfering reactions is given in Table 1. The magnitude of the interference corrections can be to a large extent controlled by a judicious choice of the irradiation time, although this approach limits production of the desired isotope (^{39}Ar), thereby reducing the measurement precision. The optimal irradiation time is thus a function of the age and the chemical composition of the sample.

One of the reactions of particular importance to very young samples is ^{40}K(n,p)^{40}Ar, which can be the dominant reaction for neutrons at thermal energies (<0.3 eV) and which produces spuriously old ages, if ignored. The correction can be significantly reduced (but not entirely eliminated) by shielding samples during irradiation with a strong thermal neutron absorber, such as cadmium (Tetley et al., 1980); this technique prevents the majority of thermal neutrons from interacting with the irradiated samples. For reactions involving fast

Table 1
Neutron capture reaction data relevant to argon isotope production from various target isotopes

Reaction	Reaction Q-value (MeV)	Reaction threshold (MeV)	Average cross section	Average (1/E)-weighted cross section	2.45-MeV cross section
^{40}K(n,nα)^{36}Cl	−10.5969 (3)	10.8861 (3)	9.01×10^{-2}	6.71×10^{-2}	
^{39}K(n,α)^{36}Cl	1.3615 (3)	0.0	2.12×10^{-1}	2.11×10^{-2}	1.53×10^{-2}
^{35}Cl(n,γ)^{36}Cl	8.57970 (7)	0.0	5.88×10^{-4}	$1.56\times10^{+2}$	9.32×10^{-4}
^{40}Ca(n,nα)^{36}Ar	−6.9912 (5)	7.1821 (5)	3.89×10^{-2}	2.86×10^{-2}	
^{36}Ar(n,γ)^{37}Ar	8.7889 (4)	0.0	1.27×10^{-3}	$1.94\times10^{+1}$	2.43×10^{-3}
^{40}Ca(n,α)^{37}Ar	1.7483 (5)	0.0	1.25×10^{-1}	1.18×10^{-2}	5.57×10^{-2}
^{37}Cl(n,γ)^{38}Cl	6.10778 (10)	0.0	3.87×10^{-4}	1.54×10^{0}	5.76×10^{-4}
^{41}K(n,α)^{38}Cl	−0.1145 (3)	0.1176 (3)	1.87×10^{-2}	5.97×10^{-3}	1.65×10^{-5}
^{40}Ar(n,t)^{38}Cl	−12.12039 (11)	12.45117 (12)	1.23×10^{-4}	1.06×10^{-4}	
^{39}K(n,d)^{38}Ar	−4.1565 (5)	4.2699 (5)	1.60×10^{-1}	1.47×10^{-1}	
^{42}Ca(n,nα)^{38}Ar	−10.3668 (4)	10.6352 (4)	1.43×10^{-1}	1.11×10^{-1}	
^{40}Ar(n,d)^{39}Cl	−10.3036 (18)	10.5774 (18)	1.44×10^{-3}	1.29×10^{-3}	
^{38}Ar(n,γ)^{39}Ar	6.598 (5)	0.0	4.61×10^{-4}	3.15×10^{0}	7.93×10^{-4}
^{42}Ca(n,α)^{39}Ar	0.341 (5)	0.0	3.07×10^{-2}	2.17×10^{-3}	2.32×10^{-4}
^{43}Ca(n,nα)^{39}Ar	−12.2011 (8)	12.5091 (8)	5.28×10^{-2}	3.96×10^{-2}	
^{40}K(n,d)^{39}Ar	−5.358 (5)	5.500 (6)	1.08×10^{-1}	1.01×10^{-1}	
^{39}K(n,p)^{39}Ar	0.217 (5)	0.0	3.21×10^{-1}	2.68×10^{-2}	1.80×10^{-1}
^{44}Ca(n,nα)^{40}Ar	−13.91 (4)	14.25 (4)	7.70×10^{-3}	5.86×10^{-3}	
^{40}K(n,p)^{40}Ar	2.2872 (3)	0.0	7.99×10^{-2}	$2.31\times10^{+1}$	3.80×10^{-2}
^{41}K(n,np)^{40}Ar	−5.5834 (3)	5.7280 (3)	3.87×10^{-2}	3.68×10^{-2}	
^{43}Ca(n,α)^{40}Ar	2.2779 (5)	0.0	2.18×10^{-2}	2.05×10^{-3}	1.59×10^{-2}

Relevant reactor-induced reactions resulting in production of argon isotopes. The cross-section data were taken from the JENDL-3 and JEF-2 300 K libraries; they were retrieved using the Evaluated Nuclear Data Files on-line database. The Q-values were calculated with the program QCALC produced by the National Nuclear Data Center of the Brookhaven National Laboratory; the uncertainty in the last figure is shown in parentheses. The average cross sections and the average ($1/E$)-weighted cross sections are specific to a ^{235}U fission spectrum; the latter (average ($1/E$)-weighted cross section) is most relevant for a first-order comparison of the relative production probabilities.

neutrons, the interference can usually be managed by minimizing irradiation duration, so that the relevant errors introduced into the calculated ages are kept below 1%. However, in extreme cases (e.g. of very young samples with a high Ca/K ratio), the interference corrections (especially those from the $^{40}Ca(n,n\alpha)^{36}Ar$ reaction) can be the accuracy-limiting factor, which compromises the correction for atmospheric ^{40}Ar.

An additional shortcoming of fission-neutron irradiation is that the resultant ^{39}Ar atoms conserve energy during the neutron capture reaction by recoiling from their original crystal–chemical site. The recoil distance is a function of the recoil energy, which in part depends on the energy spectrum of incident neutrons and on the stopping power of the medium. For neutrons in a fission spectrum, mean recoil distances of 0.08 μm have been inferred for silicates (Turner and Cadogan, 1974; Villa, 1997). Thus, materials with grain size comparable to the recoil distance may lose ^{39}Ar during irradiation, which would result in spuriously elevated $^{40}Ar/^{39}Ar$ ratios and, thus, the apparent age. Even in coarser-grained materials, ^{39}Ar recoil can be problematic due to the fractionating of ^{39}Ar from ^{40}Ar, because recoiled ^{39}Ar may be displaced into different crystal–chemical environments with retentivities different from those of ^{40}Ar. For example, if recoiled ^{39}Ar gets implanted into less thermally retentive sites, it will be released during stepwise laboratory degassing at lower temperatures, which will result in a spuriously low $^{40}Ar/^{39}Ar$ ratio and, thus, apparent age. The ^{39}Ar recoil effects are most pronounced in materials with high surface/volume ratios, such as clay minerals (e.g., Foland et al., 1992), fine-grained lavas and meteorites (e.g., Turner and Cadogan, 1974), or samples containing compositionally contrasting admixtures of phases with dimensions comparable to the recoil distance (e.g., Foland et al., 1993). Also, Onstott (1995) and Villa (1997) suggested that redistribution of ^{39}Ar due to recoil undermines the validity of the widely applied multidomain diffusion theory in K-feldspars (e.g., Lovera et al., 1989), because this theory sometimes invokes diffusion from domains whose dimensions are sufficiently small to be subject to significant recoil artifacts.

In order to minimize the recoil distance, it would be highly desirable to make the fission spectrum free of neutrons with energies above some threshold, so that the $^{39}K(n,p)^{39}Ar$ reaction would still be driven (albeit with a reduced efficiency), but the most energetic neutrons within the reaction window would be eliminated. Fig. 1 suggests that an optimal threshold for such cutoff would be in the range 2–3 MeV.

The purpose of this paper is to illustrate some of the consequences for $^{40}Ar/^{39}Ar$ dating that would follow from irradiation of samples with neutrons in this optimal energy range. Current technological developments suggest that this capability is likely to be achieved soon with high-flux deuteron–deuteron (D–D) generators. We describe one such device below.

1.1. D-D Neutron Generators

Neutron generators employing (D–D) fusion produce neutrons with energies ~2.5 MeV by the reaction $^{2}H(d,n)^{3}He$ (Csikai, 1987). The energies of D–D neutrons may be distributed, if the reaction threshold energy is substantially exceeded or the neutrons are moderated by a material in the generator. The actual energy distribution will be determined by experimental details. The existing D–D generators have been used to achieve neutron yields as high as $10^{9}\,n\,s^{-1}$ (e.g., Reijonen et al., 2004). The resulting flux depends on the geometry and sample placement, but, with the existing devices, it is difficult to achieve a flux greater than $10^{8}\,n\,cm^{-2}\,s^{-1}$, which is about four orders of magnitude lower than the fluxes of 2–3 MeV neutrons in typical fission reactors. Thus, existing D–D generators would require inordinately long irradiation times to be useful for $^{40}Ar/^{39}Ar$ dating.

A reactor of a new design (Fig. 2), which is currently under development at Lawrence Berkeley National Laboratory, is expected to generate a flux of 2.45 MeV neutrons about $10^{11}\,n\,cm^{-2}\,s^{-1}$. A neutron flux of this magnitude would be adequate for irradiating young samples (<1 Ma) for $^{40}Ar/^{39}Ar$ dating on a reasonable laboratory time scale (<50 h). The required neutron fluence varies with sample age, because the measured $^{40}Ar/^{39}Ar$ ratio must be within the mass resolution and the detector linearity range of the spectrometer, ideally between 0.01 and 100. In principle, it is possible to

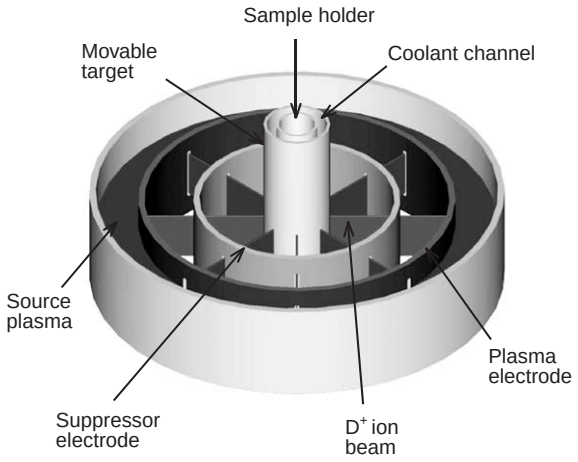

Fig. 2. A schematic diagram of a compact deuteron-deuteron neutron generator. D^{+} ions are accelerated from the toroidal source plasma chamber and implanted into the axial cylindrical Ti target, where they undergo fusion with subsequent impinging D^{+} ions. Samples for irradiation are located within the Ti target tube, which is cooled to prevent outgassing of D.

obtain a D–D neutron flux comparable to that in the relevant portion of a typical fission reactor energy spectrum, but there are practical limitations due to (1) the heat load on the target and (2) electrical power requirements. The new design features a toroidal deuteron plasma source and a coaxial self-loading deuterium-impregnated Ti target, like in the previous designs (Verbeke et al., 2000), but it differs from them in having the target rather than the source plasma chamber located centrally. In contrast with D–T reactors, whose production of $\sim$14 MeV neutrons degrades over time due to implantation of deuterons in the target, a D–D neutron generator should have a much longer useful lifetime.

In view of the prospective capability of high-flux D–D generators to produce an adequate flux of neutrons of the appropriate energies, we have investigated the effects of irradiating samples for $^{40}Ar/^{39}Ar$ dating with such neutrons. Specifically, we have modeled the production of important argon isotopes produced by reactions on K, Ca, and Cl by 2.45 MeV neutrons. In addition, we have modeled the recoil behavior of ^{39}Ar produced by neutrons of this energy. In both cases, the D–D neutrons are shown to offer significant advantages over the fission spectrum neutrons.

2. Interfering isotope corrections

Corrections for the interfering nuclear reactions are summarized in terms of the production ratios from a given target element and are specified in the format $(^{36}Ar/^{37}Ar)_{Ca}$, which indicates the $^{36}Ar/^{37}Ar$ ratio produced from all the isotopes of Ca. According to Table 1, in this case, we are dealing with the reactions $^{40}Ca(n,n\alpha)^{36}Ar$ and $^{40}Ca(n,\alpha)^{37}Ar$.

The $^{40}Ar/^{39}Ar$ age equation is commonly written as:

$$t = \frac{1}{\lambda} ln\left[1 + J\left(\frac{^{40}Ar^*}{^{39}Ar_K}\right)\right], \quad (1)$$

where $^{39}Ar_K$ denotes the ^{39}Ar produced by $^{39}K(n,p)^{39}Ar$, $^{40}Ar^*$ is the radiogenic portion of the total ^{40}Ar measured, J is a dimensionless neutron-fluence parameter determined by analysis of standards with known age, and λ is the total decay constant for ^{40}K. Interference corrections come into play in determining $^{40}Ar^*$ and $^{39}Ar_K$ from the total measured isotope abundances $^{40}Ar_m$ and $^{39}Ar_m$ as described below.

Neglecting the trivial production of ^{40}Ar from Ca, we must take into account the reactor-produced contribution from K ($^{40}Ar_K$) and atmospheric contamination ($^{40}Ar_A = 296 \times {}^{36}Ar_A$):

$$^{40}Ar^* = {}^{40}Ar_m - {}^{40}Ar_K - {}^{40}Ar_A. \quad (2)$$

With the additional corrections for $^{40}Ca(n,n\alpha)^{36}Ar$, Eq. (2) can be rewritten as

$$^{40}Ar^* = {}^{40}Ar_m - {}^{39}Ar_K - 296\left[{}^{36}Ar_m - {}^{37}Ar_{Ca}\left(\frac{^{36}Ar}{^{37}Ar}\right)_{Ca}\right], \quad (3)$$

where ^{37}Ar must be corrected for the radioactive decay since irradiation. Determining $^{39}Ar_K$ is more straightforward, it requires only a correction for $^{39}Ar_{Ca}$:

$$^{39}Ar_K = {}^{39}Ar_m - {}^{37}Ar_{Ca}\left(\frac{^{39}Ar}{^{37}Ar}\right)_{Ca}. \quad (4)$$

Eqs. (2)–(4) ignore the reactor-produced Ar isotopes from Cl, which are normally negligible due to the low Cl content of most samples. The most significant Cl-derived isotope in terms of the effect on the age equation is $^{36}Ar_{Cl}$, whose formation due to the β^- decay of reactor-produced ^{36}Cl ($t_{1/2}$ $\sim 3 \times 10^5$ y) is too slow to be significant in a period of time typically needed for an analysis. Note that ^{38}Cl decays by β^- emission to ^{38}Ar with a half-life of $\sim$37 min, and ^{39}Cl decays by β^- emission to ^{39}Ar with a half life of $\sim$56 min.

The interference corrections (isotope production ratios) appearing in Eqs (2)–(4) and several others of interest are determined from analyses of simple synthetic compounds. Values determined from multiple irradiations performed over 10 y in the cadmium-lined in-core irradiation tube (CLICIT) facility at the Oregon State University Triga (OSTR) reactor are summarized in Table 2. These values may vary from one reactor to another and even from one irradiation to another in a given reactor, particularly where the relevant cross-section functions are most disparate energetically. For example, the value of $(^{40}Ar/^{39}Ar)_K$, which involves both fast and thermal neutrons for the $^{39}K(n,p)^{39}Ar$ and $^{40}K(n,p)^{40}Ar$ reactions, respectively, is known to vary by several orders of magnitude between reactors and somewhat less between fueling cycles in a given reactor (McDougall and Harrison, 1999).

Table 2 shows estimated production ratios for 2.45 MeV neutrons; the ratios have been calculated from the values listed in Table 1 and weighted by isotope abundances. As compared with the fission-spectrum neutrons (used with or without Cd shielding), D–D neutrons eliminate the $(^{37}Ar/^{39}Ar)_K$, $(^{36}Ar/^{37}Ar)_{Ca}$, and $(^{38}Ar/^{37}Ar)_{Ca}$ corrections; they also reduce the other corrections from K and Ca by one or more orders of magnitude. This allows to use the irradiation time for a production of $^{39}Ar_K$ that would provide desired measurement precision without an excessive generation of the unwanted isotopes, such as $^{36}Ar_{Ca}$. This holds promise for a much greater accuracy in dating of young, low-K high-Ca/K, materials, such as plagioclase. Fig. 3 illustrates the modeled effects of the interference corrections on the error in the calculated age of a

Table 2
Argon isotope production ratios

Production ratio	D–D neutrons (2.45 MeV)	Fission-spectrum neutrons (Cd-shielded)[a,b,c]	Fission-spectrum neutrons (unshielded)[d,e]
$(^{40}Ar/^{39}Ar)_K$	3.86×10^{-6}	$(7.30 \pm 0.92) \times 10^{-4}$	$(4.6 \pm 0.5) \times 10^{-3}$
$(^{38}Ar/^{39}Ar)_K$[f]	6.64×10^{-6}	$(1.22 \pm 0.00) \times 10^{-2}$	
$(^{37}Ar/^{39}Ar)_K$	0	$(2.24 \pm 0.16) \times 10^{-4}$	
$(^{36}Ar/^{37}Ar)_{Ca}$	0	$(2.65 \pm 0.02) \times 10^{-4}$	$(2.68 \pm 0.04) \times 10^{-4}$
$(^{38}Ar/^{37}Ar)_{Ca}$	0	$(1.96 \pm 0.08) \times 10^{-5}$	
$(^{39}Ar/^{37}Ar)_{Ca}$	2.78×10^{-5}	$(6.95 \pm 0.09) \times 10^{-4}$	$(6.98 \pm 0.63) \times 10^{-4}$
$(^{36}Ar/^{38}Ar)_{Cl}$[g]	$5.06 \times f(t)$		$(3.21 \pm 0.02) \times 10^{2} \times f(t)$

Production ratios for D–D neutrons have been estimated using values from Table 1. Unshielded fission-spectrum production ratios are for the Ca- and K-derived isotopes in the OSTR reactor [d] and for the Cl-derived isotopes in the Herald reactor[e].

[a] Renne et al. (1998).

[b] Renne and Norman (2001).

[c] Knight et al. (2003).

[d] Wijbrans et al. (1995).

[e] Roddick (1983).

[f] In the case of the D–D neutrons, $^{38}Ar_K$ comes only from the reaction $^{41}K(n,\alpha)^{38}Cl \rightarrow ^{38}Ar$ ($t_{1/2} = 37$ m), whereas, in the case of the fission-spectrum neutrons, it is predominantly from the reaction $^{39}K(n,d)\ ^{38}Ar$.

[g] $^{36}Ar_{Cl}$ comes from the reaction $^{35}Cl(n,\gamma)\ ^{36}Cl \rightarrow ^{36}Ar$ ($t_{1/2} = 2.95 \times 10^5$ yr), and $^{38}Ar_{Cl}$ comes from the reaction $^{37}Cl(n,\gamma)\ ^{38}Cl \rightarrow ^{38}Ar$ ($t_{1/2} = 37$ m). The ratio is therefore time dependent, with t given in days (d) and $f(t) = [(1 - e^{At})/(1 - e^{Bt})]$ where $A = -6.427 \times 10^{-9}\ d^{-1}$, $B = -26.8\ d^{-1}$.

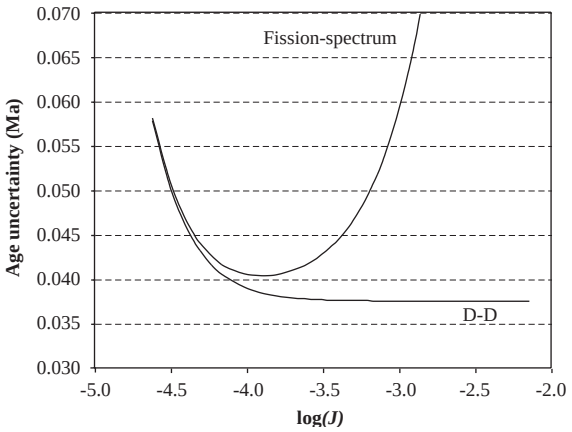

Fig. 3. Uncertainties in the results of age determination with D–D and fission-spectrum neutrons at various J values (J is a dimensionless neutron-fluence parameter linearly correlated with the irradiation time). The results have been obtained by modeling based on propagating the interference corrections (production ratios listed in Table 2) through Eq. (1) for 10 g of 100-ka plagioclase with 10^{-12} mol g^{-1} atmospheric ^{40}Ar, 0.25% K and Ca/K = 50, analyzed 3 months after irradiation.

10^5-yr old (100 ka) plagioclase sample for the D–D and fission-spectrum neutrons. It shows that, with a D–D irradiation, the error asymptotically approaches a value that is significantly smaller than the minimum error achievable with a fission-spectrum neutron irradiation. Fig. 3 also illustrates the existence of an optimal fluence for a fission-spectrum irradiation (in this case, at $J = 0.00013$, corresponding to 0.55 h), which is not the case for D–D irradiations.

The use of D–D neutrons reduces $(^{40}Ar/^{39}Ar)_K$ by two or more orders of magnitude, rendering this correction negligible. The $(^{37}Ar/^{39}Ar)_K$ value is eliminated, and $(^{39}Ar/^{37}Ar)_{Ca}$ is reduced by an order of magnitude, thereby allowing ^{37}Ar and ^{39}Ar to be taken straightforwardly as proxies for Ca and K, respectively, without the need to propagate errors through simultaneous equations (Renne, 2000). Thus, useful compositional information about samples can still be obtained, like in the case of the activation by fission-spectrum neutrons, but without the undesired collateral interferences.

For a given mass spectrometry and gas extraction system, the optimal neutron fluence depicted in Fig. 3 for fission-spectrum irradiation varies as a function of sample age, chemical composition, and mass. For practical and financial reasons, it is common to irradiate many samples together, which requires a compromise in the irradiation time. In contrast, there is no optimum fluence of D–D neutrons for the minimal error introduced by the interference corrections. Thus, there is no evident penalty for overirradiating samples (provided that the resulting argon isotope ratios are within the mass resolution tolerances) and coirradiating samples with disparate ages and compositions involves no such compromise.

Irradiation with D–D rather than fission-spectrum neutrons would also help the analysis of data in the cosmic radiation dosimetry based on the approach

developed by Turner et al. (1971). This technique uses measurements of the natural spallogenic ^{38}Ar ($^{38}Ar_{cos}$) produced from either Ca or K and compares them with neutron activation proxies ($^{37}Ar_{Ca}$ or $^{39}Ar_{K}$, respectively) for the target element. Elimination of the interfering reaction $(^{38}Ar/^{37}Ar)_{Ca}$ and reduction of $(^{38}Ar/^{39}Ar)_{K}$ by four orders of magnitude (Table 2) dramatically reduce the corrections necessary to determine $^{38}Ar_{cos}$. This benefit is especially pronounced in the case of long irradiations, which are usual when cosmic radiation dosimetry data are sought as a corollary to data used for $^{40}Ar/^{39}Ar$ dating of old extraterrestrial materials of limited availability.

3. Recoil energy and distance

Recoil displacement produces depletion profiles, wherein ^{39}Ar is preferentially ejected near grain boundaries. We have calculated ^{39}Ar depletion profiles for an isotropic flux of incident neutrons corresponding to the D–D and fission-spectrum energies. We used the most recent version of the SRIM 2003 code (http://www.srim.org/) including the program transport of ions through matter (TRIM) to calculate the stopping range of the recoiled ^{39}Ar as a function of the angle of attack and the energy of this atom. TRIM (based on the book by Ziegler et al., 1985) utilizes the Monte Carlo method to track the collision histories of a large number of incident "attacking" particles (1000 ^{39}Ar atoms in our case). In our calculations, we used an amorphous target of annite composition (Fe-rich trioctahedral mica, $KFe_3(AlSi_3)O_{10}(OH)_2$). In the simulations, we assumed the lattice binding energies equal to 3 eV for K, Al, Fe, O, H, and 2 eV for Si, displacement energies equal to 25 eV for K, Al, and Fe; 15 eV for Si; 28 eV for O, and 10 eV for H, and the density of the material equal to 3.22 g/cm^3. The recoil energy of ^{39}Ar used in our model was 57.5 keV; it was calculated as the maximum recoil energy possible from 2.45 MeV neutrons and constituted approximately 32% of the mean energy of ^{39}Ar produced by the fission-spectrum neutrons (177 keV; Onstott et al., 1995). The energy of recoiling atoms ($m/e = 38.962$ in our case) is reduced by nuclear collision (elastic), electronic collision (inelastic), and losses to phonons. Simulations were run for various annite slab thicknesses over ejection angles ranging between 0–90° (in 5° steps).

Fig. 4 shows the simulation results for annite. As expected, the lower recoil energy spectrum produced by the D–D neutrons results in significantly lower depletion of ^{39}Ar. Recoil displacement is essentially a function of chemical composition, and other silicates yield profiles very similar to that for annite. For comparison, the recoil range (mean displacement distance) determined for various minerals used in $^{40}Ar/^{39}Ar$ geochronology

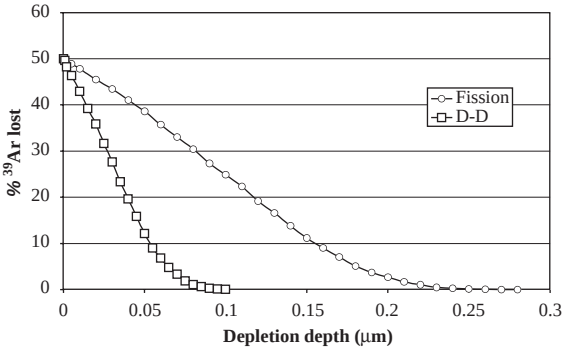

Fig. 4. Depletion of ^{39}Ar from a semi-infinite slab of annite deduced from SRIM for ^{39}Ar created by an isotropic flux of fission spectrum (circles) and D–D (squares) neutrons. See text for modeling details.

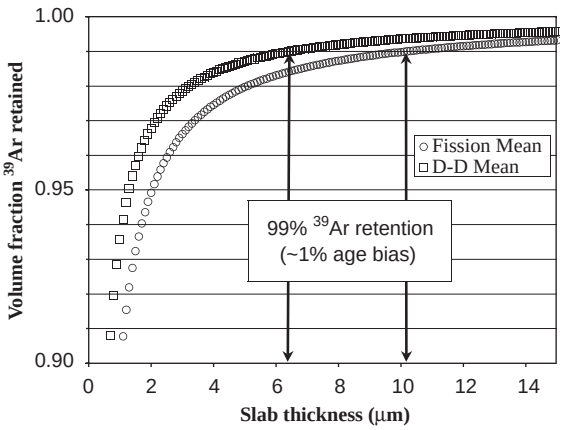

Fig. 5. Volume fraction of ^{39}Ar retained at different depths of an infinite slab of an annite composition. Squares: ^{39}Ar created by the fission-spectrum neutrons; circles: ^{39}Ar created by the D–D neutrons. The arrows show slab thickness corresponding to 99% ^{39}Ar retention, which translates into ~1% excess age bias. The figure is based on the SRIM simulation data shown in Fig. 4.

varied from 0.14 (magnesiohornblende $Ca_2Mg_4Fe_{0.25}Al_{1.75}Si_7O_{22}(OH)2$, $d = 3.23\,g\,cm^{-3}$) to 0.18 μm (Leucite $KAlSi_2O_6$, $d = 2.46\,g\,cm^{-3}$) for the fission-spectrum neutrons, but only from 0.05 to 0.06 μm for the same minerals irradiated by the D–D neutrons.

The age bias due to recoil depends on the volume fraction of ^{39}Ar lost from mineral grains. The fraction of ^{39}Ar depleted from crystal margins depend on their shape, and particularly on the surface/volume ratio. The effects are especially severe for platy minerals, such as micas and clays. As shown in Fig. 5 for infinite slab geometry, the minimum slab thickness for >99% ^{39}Ar retention (i.e., <1% age bias) is about 6.5 μm with the D–D neutrons, and 10.2 μm with the fission-spectrum

neutrons. For more stringent bias criteria (i.e., for a greater than 99% ^{39}Ar retention), the difference between the slab thickness thresholds increases. For 99.5% retention, the requirements are 12.9 μm with the D–D neutrons and 20.3 μm with the fission-spectrum neutrons.

4. Radiological considerations

Aluminum is an abundant element in many geologic samples; it is also a desirable sample holder material due to its low elastic scattering cross section. Unfortunately, the large $^{27}Al(n,\alpha)^{24}Mg$ cross section for fission-spectrum neutrons raises radiological concerns because of the radiation from the $^{24}Mg \rightarrow {}^{24}Na\ \beta^-$ decay ($t_{1/2}$= 15 h). With fission reactors, the post irradiation cooling of activated Al necessary for radiological purposes is often ~2 weeks or more. The $^{27}Al(n,\alpha)^{24}Mg$ reaction has a negligible cross section for the D–D neutrons, which eliminates the $^{24}Mg\ \beta^-$decay and allows a faster and safer analysis of the samples.

5. Conclusions

For most $^{40}Ar/^{39}Ar$ dating, irradiation with ~2.5 MeV neutrons offers significant advantages over conventional irradiation with neutrons from a ^{235}U fission spectrum. Interference corrections are reduced or eliminated without a loss of the important geochemical tracers $^{37}Ar_{Ca}$ and $^{38}Ar_{Cl}$. The unfavorable consequences of over irradiation are removed, which provides much wider latitude in choosing the irradiation time. Recoil displacement of ^{39}Ar is significantly reduced, which results in a lower grain size threshold for age artifacts. Elimination of the $^{27}Al(n,\alpha)^{24}Mg$ reaction reduces radiological concerns about handling samples soon after irradiation. In short, there are many benefits and no obvious drawbacks in using ~2.5 MeV neutrons for $^{40}Ar/^{39}Ar$ dating instead of the fission-spectrum ones.

A D–D fusion device producing essentially monoenergetic (2.45 MeV) neutrons appears capable of producing adequately high neutron fluxes to be useful for $^{40}Ar/^{39}Ar$ dating. A promising design for such a device features a toroidal deuterium plasma source, a centrally located hollow cylindrical Ti target, which self-loads with implanted deuterons, and samples placed inside the target cylinder. Whether or not this particular design serves the purpose, we anticipate that D–D fusion research will almost certainly produce such capabilities. The scientific benefits for $^{40}Ar/^{39}Ar$ dating are sufficient to justify an effort to construct and test such devices, particularly in view of the low cost of construction and operation, as compared with fission reactors.

Acknowledgements

We thank S. Prussin and P. Petersen for helpful suggestions and discussion; K. Ludwig, V. Nagy, and two anonymous reviewers for constructive comments on the manuscript.

References

Csikai, J., 1987. CRC Handbook of Fast Neutron Generators. Vol. 1. CRC Press, Florida 242pp.

Foland, K.A., Fleming, T.H., Heimann, A., Elliot, D.H., 1993. Potassium argon dating of fine-grained basalts with massive Ar loss—application of the $^{40}Ar/^{39}Ar$ technique to plagioclase and glass from the Kirkpatrick basalt, Antarctica. Chem. Geol. 107, 173–190.

Foland, K.A., Hubacher, F.A., Arehart, G.B., 1992. $^{40}Ar/^{39}Ar$ dating of very fine-grained samples—an encapsulated-vial procedure to overcome the problem of Ar recoil loss. Chem. Geol. 102, 269–276.

Garner, E.L., Murphy, T.J., Gramlich, J.W., Paulsen, P.J., Barnes, I.L., 1975. Absolute isotopic abundance ratios and the atomic weight of a reference sample of potassium. J. Res. Natl. Bureau Stand. 79A, 713–725.

Humayun, M., Clayton, R.N., 1995. Precise determination of the isotopic composition of potassium: application to terrestrial rocks and lunar soils. Geochim. Cosmochim. Acta 59, 2115–2130.

Knight, K.B., Renne, P.R., Halkett, A., White, N., 2003. $^{40}Ar/^{39}Ar$ dating of the Rajahmundry Traps, Eastern India, and their relationship to the Deccan Traps. Earth Planet. Sci. Lett. 208, 85–99.

Lovera, O.M., Richter, F.M., Harrison, T.M., 1989. The $^{40}Ar/^{39}Ar$ thermochronometry for slowly cooled samples having a distribution of diffusion domain sizes. J. Geophys. Res. 94, 17917–17935.

McDougall, I., Harrison, T.M., 1999. Geochronology and Thermochronology by the $^{40}Ar/^{39}Ar$ Method. Oxford University Press, Oxford 269 pp.

Merrihue, C., Turner, G., 1966. Potassium–argon dating by activation with fast neutrons. J. Geophys. Res. 71, 2852–2857.

Onstott, T.C., Miller, M.L., Ewing, R.C., Arnold, G.W., Walsh, D.S., 1995. Recoil refinements: implications for the $^{40}Ar/^{39}Ar$ dating technique. Geochim. Cosmochim. Acta 59, 1821–1834.

Reijonen, J., Leung, K.-N., Firestone, R.B., English, J.A., Perry, D.L., Smith, A., Gicquel, F., Sun, M., Koivunoro, H., Lou, T.-P., Bandong, B., Garabedian, G., Revay, Zs., Szentmiklosi, L., Molnar, G., 2004. First PGAA and NAA experimental results from a compact high intensity D–D neutron generator. Nucl. Instr. Methods Phys. Res. A 522, 598–602.

Renne, P.R., 2000. K-Ar and $^{40}Ar/^{39}Ar$ Dating, Quaternary Geochronology: methods and applications. In: Noller, J.S., Sowers, J.M., Lettis, W.R. (Eds.), American Geophysical Union Reference Shelf Series, Vol. 4. Ameerican Geophysical Union, Washington DC, pp. 77–100.

Renne, P.R., Norman, E.B., 2001. Determination of the half-life of ^{40}Ar by mass spectrometry. Phys. Rev. C 63 (047302), 3.

Renne, P.R., Sharp, W.D., Deino, A.L., Orsi, G., Civetta, L., 1997. $^{40}Ar/^{39}Ar$ dating into the historical realm: calibration against pliny the younger. Science 277, 1279–1280.

Renne, P.R., Swisher, C.C., Deino, A.L., Karner, D.B., Owens, T., DePaolo, D.J., 1998. Intercalibration of standards, absolute ages and uncertainties in $^{40}Ar/^{39}Ar$ dating. Chem. Geol. (Isotope Geosci. Sect.) 145 (1–2), 117–152.

Roddick, J.C., 1983. High precision intercalibration of ^{40}Ar–^{39}Ar standards. Geochim. Cosmochim. Acta 47, 887–898.

Turner, G., 1971. Argon 40—argon 39 dating: the optimization of irradiation parameters. Earth Planet. Sci. Lett. 10, 227–234.

Turner, G., Cadogan, P., 1974. Possible effects of ^{39}Ar recoil in ^{40}Ar–^{39}Ar dating. Proceedings of the 5th Lunar and Planetary Science Conference, 1601–1615.

Turner, G., Huneke, J.C., Podosek, F.A., Wasserburg, G.J., 1971. ^{40}Ar-^{39}Ar ages and cosmic ray exposure ages of Apollo samples. Earth Planet. Sci. Lett. 12, 19–35.

Tetley, N., McDougall, I., Heydegger, H.R., 1980. Thermal neutron interferences in the $^{40}Ar/^{39}Ar$ dating technique. J. Geophys. Res. B 85, 7201–7205.

Verbeke, J.M., Leung, K.-N., Vujic, J., 2000. Development of a sealed-accelerator-tub neutron generator. Appl. Radiat. Isot. 53, 801–809.

Villa, I.M., 1997. Direct determination of ^{39}Ar recoil distance. Geochim. Cosmochim. Acta 61, 689–691.

Wijbrans, J.R., Pringle, M.S., Koppers, A.A.P., Scheveers, R., 1995. Argon Geochronology of Small Samples Using the Vulkaan Argon Laser-Probe. K. Ned. Acad. Wet. (Amsterdam) 98, 185–218.

Ziegler, J.F., Biersack, J.P., Littmark, U., 1985. The Stopping and Range of Ions in Solids. Pergamon Press, New York.